

R-L 負荷에 對한 交流電流 制御方式

論	文
29-12-1	

A.C. Current Control Scheme for R-L Load

朴 旻 鎬* · 崔 圭 夏**

(Min-Ho Park · Gyu-Ha Choe)

Abstract

This paper is concerned with the study of improving the faults of phase control scheme and suggesting a new approach to the control of load circuit with AC source. AC current control can restrict the magnitude of current within the given upper and lower current and make current continuous during every cycle.

Also the harmonic contents of current can be greatly reduced using this control scheme. Analog computer and digital computer simulations reveal that the current control scheme is superior to the phase control scheme in controlling the power supply to the load R-L. Experimental results demonstrate the feasibility and verify the operation of current controlled system.

I. Introduction^{1,2,3,4)}

Of the control scheme using thyristor switches, phase control is commonly used for the voltage control of load circuit and the output power can be controlled easily as advancing or retarding the firing angle. The phase control scheme has the disadvantages as follows:

- 1) In R-L load, as the firing angle must be given in the range greater than the phase angle of load, the control range becomes reduced.
- 2) The load current is always discontinuous under any load condition.
- 3) The ratio of the peak to the rms value of current is increased in the system of low load impedance, for the conduction angle becomes decreased as the firing angle increases.
- 4) Also, as the harmonic contents of load

current increase with the firing angle, the current ratio (K_r , defined in Eq.(20)) decreases and the output waveform worsens i.e., the the distortion factor (K_d defined in Eq.(21)) becomes greater.

To improve the above faults, AC current control scheme for R-L load system is suggested here. In AC current control scheme, the load current can be operated in the continuous mode and the harmonic contents of the load current can be controlled using the limit currents of sine wave. Digital computation, analog computer and the experimental set-up are made to demonstrate and to analyze AC current controlled system.

II. AC Current Control Scheme

AC current control scheme is represented as the multiple ON-OFF control during each cycle of the source. The load current is sensed through the current sensor and compared with the upper and lower limit current of the comparator circuit

* 正會員: 서울大 工大 電氣工學科 教授 · 工博

** 正會員: 建國大 工大 電氣工學科 專任講師

接受日字: 1980年 9月 17日

and then the load system is controlled by the ON-OFF signals generated from the comparator.

Fig. 1-a, b shows power circuit and the block diagram of the control circuit of this control scheme for R-L load. And the output waveforms are given in Fig. 1-c.

A. Operation

AC current control scheme is described by the following two modes, one mode which the load current rises to the upper limit i_u and the other which the current falls to the lower limit i_L . The basic operation of this scheme is the same as that of Jones chopper circuit.⁵⁾

1) Mode I

Interval a of Fig. 1-c is represented as one of these modes. As the ON signal turns on the thyristor T_1' , the load is connected to the source and load current rises.

At the same time, the commutating capacitor C_1 is charged by the autotransformer AT to turn off T_1' at the next mode. When the load current reaches the upper limit i_u , the OFF signal is generated from the comparator.

By the OFF signal, the auxiliary T_1^b is turned on.

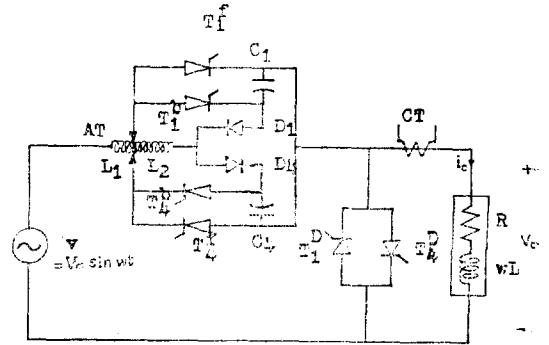
From this time turned off the main thyristor, the Mode II is started.

2) Mode II

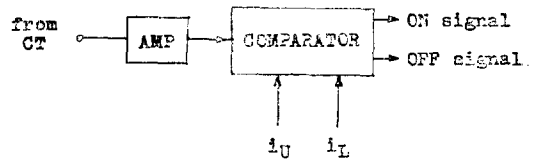
Interval b of Fig. 1-c is shown as one of these modes.

When the OFF signal turns on the auxiliary thyristor T_1^b , the energy charged in C_1 is discharged and so load current begins to decay through the free wheeling thyristor T_1^p . If the diodes are used as the free wheeling path, then circuit is shorted through diodes because of the polarity of the source. As the load current falls below the lower i_L , the load is reconnected to the source and the load current rises again. Also the operation returns to the Mode I again. In negative cycle of source, these operations are the same.

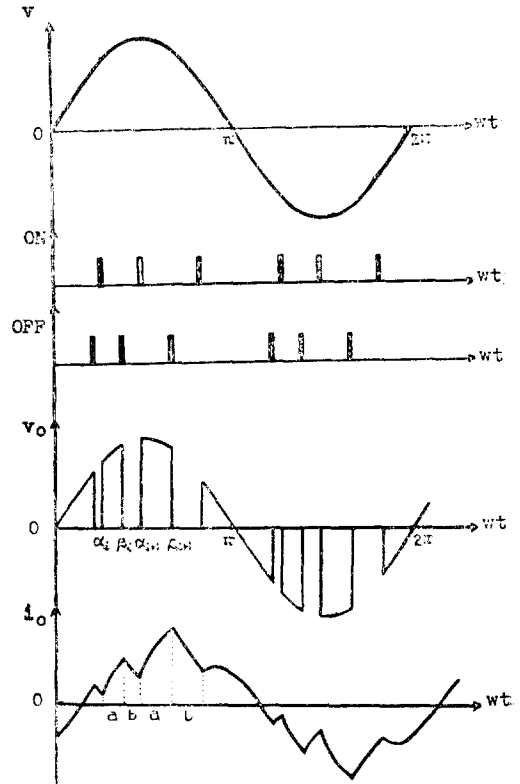
While repeating the above operations, AC current control scheme uses both the forced commutation and the natural commutation to turn



(a) Power circuit



(b) Control circuit



(c) Output waveforms

Fig. 1. AC current controlled system.

off the thyristors. In the Mode II, the forced commutation is used to turn off the main thyristors and at the beginning of the Mode I the free wheeling thyristors are commutated by the polarity of the source, when the main thyristor is ON again. In AC current control scheme, the upper and lower limit currents of the comparator are given in the following forms:

$$i_U = I_{MU} \sin(\omega t - \theta_R) \quad (1)$$

$$i_L = I_{ML} \sin(\omega t - \theta_R) \quad (2)$$

AC current control has the characteristic of forming the limit currents as the sine wave and this becomes the key-point to improve the system performance better than that of the phase control.

B. Derivation of the EQS. for Each Mode

1) Mode I ($\alpha_i \leq \omega t \leq \beta_i$)

For each cycle, the operation of Mode I repeats succeedingly until the polarity of the source changes.

At $\omega t = \alpha_i$, the load is connected to the source and the load current begins to rise from the value of the lower limit i_L . The Eq. of this Mode is as follows:

$$V_m \sin \omega t = L \frac{di_o}{dt} + Ri_o \quad (3)$$

Laplace transform on both sides of Eq. (1) gives

$$i_o(s) = \frac{\omega V_m / L}{(s + R/L)(s^2 + \omega^2)} + \frac{I(0)}{s + R/L} \quad (4)$$

where $I(0)$ is the initial value of current.

Taking the inverse Laplace transform of Eq.(2),

$$i_o(\omega t) = \frac{\omega L \cdot V_m}{R^2 + \omega^2 L^2} e^{-\frac{R}{\omega L} \omega t} + I(0) e^{-\frac{R}{\omega L} \omega t} + \frac{V_m}{\sqrt{R^2 + \omega^2 L^2}} \sin\left(\omega t - \tan^{-1} \frac{\omega L}{R}\right) \quad (5)$$

At $\omega t = \alpha_i$, as the load current arrives at the lower limit i_L ,

$$i_o(\alpha_i) = i_L(\alpha_i) \quad (6)$$

From Eq. (5) and (6), the initial value $I(0)$ can be obtained as:

$$I(0) = i_L(\alpha_i) e^{\frac{R}{\omega L} \alpha_i} - \frac{\omega L \cdot V_m}{R^2 + \omega^2 L^2} - \frac{V_m}{\sqrt{R^2 + \omega^2 L^2}} e^{\frac{R}{\omega L} \alpha_i}$$

$$\cdot \sin\left(\alpha_i - \tan^{-1} \frac{\omega L}{R}\right) \quad (7)$$

Substituting the Eq. of initial value from Eq. (7) in Eq. (5), the instantaneous load current of Mode I is derived as:

$$i_o(\omega t) = \frac{V_m}{\sqrt{R^2 + \omega^2 L^2}} \sin\left(\omega t - \tan^{-1} \frac{\omega L}{R}\right) + i_L(\alpha_i) e^{-\frac{R}{\omega L}(\omega t - \alpha_i)} - \frac{V_m}{\sqrt{R^2 + \omega^2 L^2}} \cdot \sin\left(\alpha_i - \tan^{-1} \frac{\omega L}{R}\right) e^{-\frac{R}{\omega L}(\omega t - \alpha_i)} \quad (8)$$

Also the load voltage is given by:

$$v_o(\omega t) = V_m \sin \omega t \quad (9)$$

2) Mode II ($\beta_i \leq \omega t \leq \alpha_{i+1}$)

When the load current reaches the upper limit i_U , the load is disconnected from the source and the load current decays through the free wheeling path. The Eq. of the Mode II is derived as follows:

$$0 = L \frac{di_o}{dt} + Ri_o \quad (10)$$

At $\omega t = \beta_i$, as the load current expressed by Eq. (8) arrives at the the upper limit, the initial value $I(0)$ of Mode II is given by:

$$I(0) = i_o(\beta_i) = i_U(\beta_i) \quad (11)$$

From Eq. (10) and (11), Eqs. of the load current and voltage can be obtained as:

$$i_o(\omega t) = i_U(\beta_i) e^{-\frac{R}{\omega L}(\omega t - \beta_i)} \quad (12)$$

$$v_o(\omega t) = 0 \quad (13)$$

The Eqs. of the load current and voltage derived in each Mode are used to analyze the AC current control scheme by digital computations.

III. Digital Computations

Based on the above Eqs., digital computer is used to obtain a theoretical description of the system performance and the flow chart is given in Fig. 2. The output current and voltage waveforms obtained from the digital computer are in Fig. 3-a. Also the rms value, the harmonic contents and the distortion factor of load current are computed digitally in each case of $i_{DF} = 0.1 \sim 0.6$ pu (per unit; here, 1 pu = 2.93A).

A. RMS Value of Load Current

Fig. 4 shows the changes of rms values to various lower limit i_L for each case of $i_{DF}=0.1 \sim 0.6$ pu. It can be found that the load current is increased as i_L is increased and i_{DF} is increased in a fixed i_L . Also as the upper limit i_U is increased, the rms value is increased and the control range becomes wider.

B. Current Ratio

To investigate the harmonic contents of load current, the load current can be described by the Fourier series.

$$i_o(\omega t) = \sum_{n=1}^{\infty} (a_n \sin n\omega t + b_n \cos n\omega t) \quad (14)$$

$$\begin{aligned} \text{where } a_n &= \frac{2}{\pi} \int_0^{\pi} i_o(\omega t) \sin n\omega t \, d\omega t & (15) \\ &= \frac{2}{\pi} \left[\int_{\alpha_0}^{\beta_0} i_o(\omega t) \sin n\omega t \, d\omega t \right. \\ &\quad \left. + \int_{\beta_0}^{\alpha_1} i_o(\omega t) \sin n\omega t \, d\omega t + \dots \right] & (16) \end{aligned}$$

and

$$\begin{aligned} b_n &= \frac{2}{\pi} \int_0^{\pi} i_o(\omega t) \cos n\omega t \, d\omega t & (17) \\ &= \frac{2}{\pi} \left[\int_{\alpha_0}^{\beta_0} i_o(\omega t) \cos n\omega t \, d\omega t \right. \\ &\quad \left. + \int_{\beta_0}^{\alpha_1} i_o(\omega t) \cos n\omega t \, d\omega t + \dots \right] & (18) \end{aligned}$$

The rms value of the n-th harmonic is then given by:

$$I_n = \frac{1}{\sqrt{2}} \sqrt{a_n^2 + b_n^2} \quad (19)$$

From the above Eqs., the current ratio K_{cr} is defined as:

$$K_{cr} = \frac{I_1}{\sqrt{I_1^2 + I_3^2 + I_5^2 + \dots}} = \frac{I_1}{\sqrt{\sum I_n^2}} \quad (20)$$

Here the rms value of the 7-th harmonic is considered in computing digitally. From Fig. 5, as the lower limit i_L is increased in a constant i_{DF} and as i_{DF} is decreased, the harmonic content of load current is reduced and the current ratio approaches to about unity. Therefore it can be known that there are included little harmonic contents in the load current.

C. Distortion Factor

When AC current control scheme used, the various values of the distortion factor are shown in Fig. 6 and the distortion factor K_d can be defined as follows:

$$K_d = \frac{\sqrt{\sum I_n^2 - I_1^2}}{I_1} \quad (21)$$

From Fig. 6, it can be found that as i_{DF} is decreased and i_L is increased in a constant value of i_{DF} , K_d is decreased and the output current waveform becomes close to the sine wave.

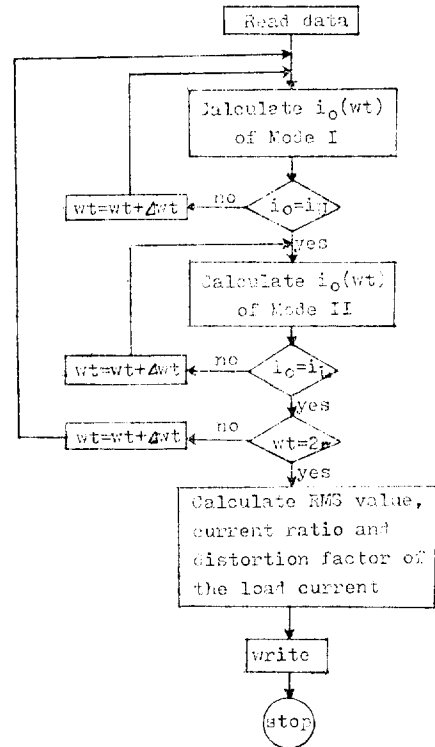


Fig. 2. Flow chart of AC current controlled system

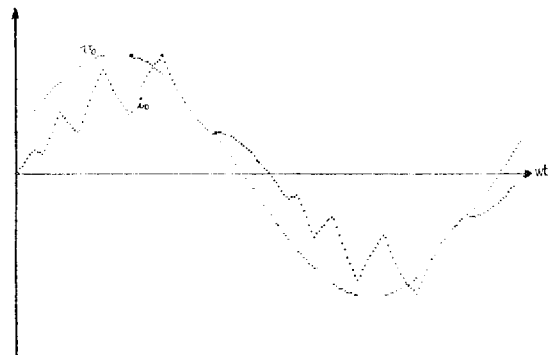


Fig. 3. Output waveforms obtained from digital computer ($i_U=0.65$ pu, $i_L=0.35$ pu, $i_o=0.52$ pu)

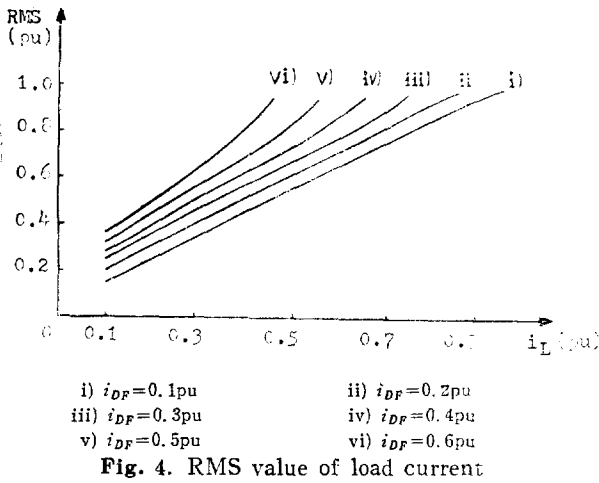


Fig. 4. RMS value of load current

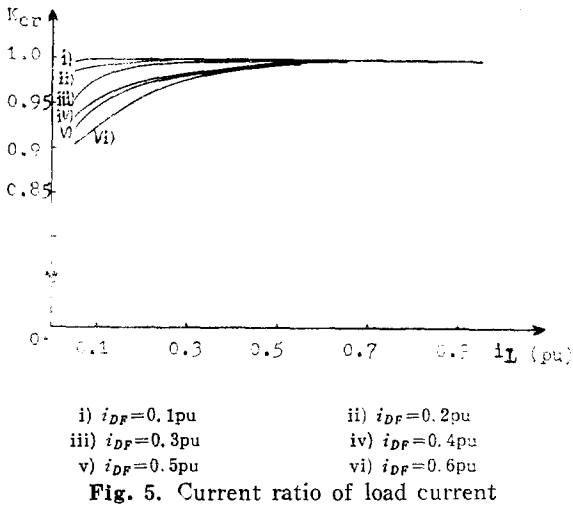


Fig. 5. Current ratio of load current

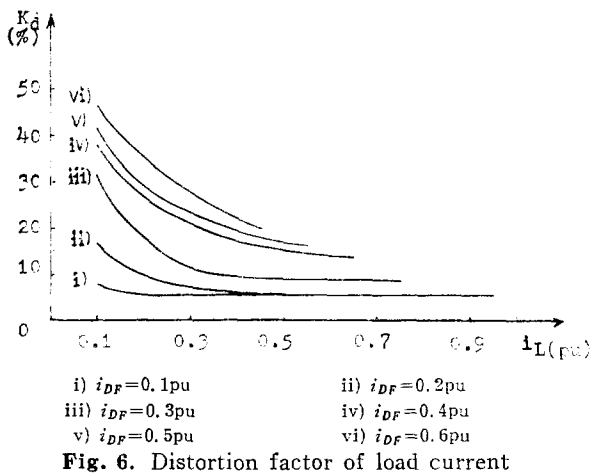


Fig. 6. Distortion factor of load current

IV. Experimental Results

A. Analog Computer Set-Up

AC current controlled system is simulated on analog computer by the following Eq. from Eq. (3).

$$\frac{di_o}{dt} = -\frac{V_m}{L} \sin \omega t - \frac{R}{L} i_o \quad (22)$$

A 60Hz sine wave oscillator is used as an analog for the AC source. The multiplier is used as an analog for thyristor switch and the control logic signal from OR gate as the analog of the gating signals. Also the phase shifter is used to control the upper and lower limit currents close to the phase angle. With AND operation of the Z.C. output and F/F output, ON_p is supplied only at the positive cycle and ON_n is only at the negative cycle of source to the multiplier. The complete analog computer simulation of AC current controlled system is given in Fig. 7. Fig. 8 shows the results from analog computer set-up. The analog simulation reveals that the load current can be made continuous and the harmonic contents can be controlled by changing the upper and lower limit current.

B. Experimental Set-Up

The circuits of Fig. 1-a, b are used as the experimental set-up to demonstrate the feasibility of the AC current controlled system. The load current is sensed through the current sensor CT and it is amplified by the AMP and the two

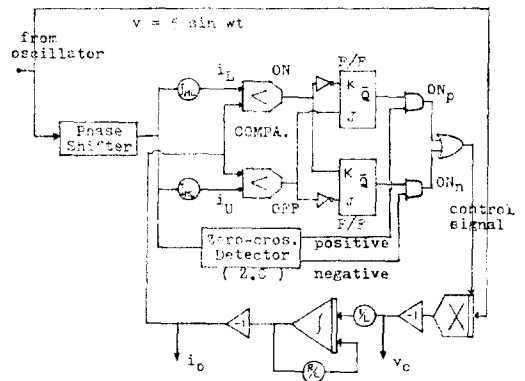
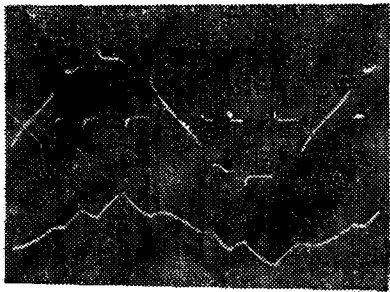
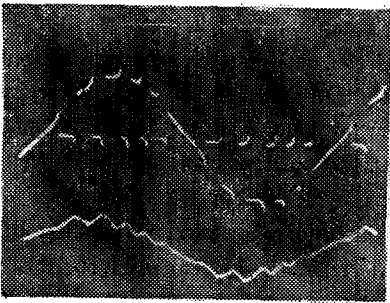


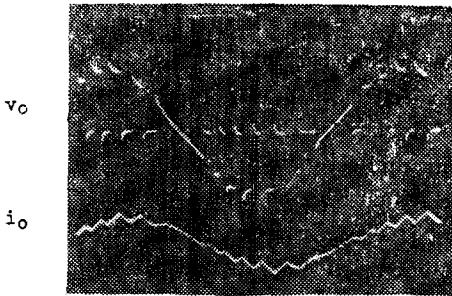
Fig. 7. Analog computer set-up of the AC current controlled system



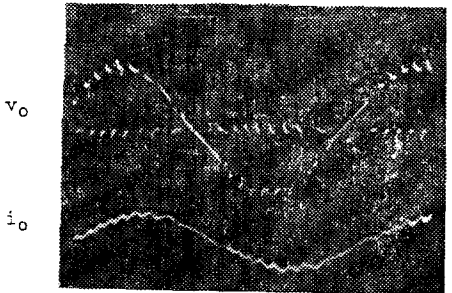
(a) $i_U = 0.8 \text{ pu}$ $i_o = 0.5 \text{ pu}$
 $i_L = 0.35 \text{ pu}$



(b) $i_U = 0.8 \text{ pu}$ $i_o = 0.67 \text{ pu}$
 $i_L = 0.5 \text{ pu}$



(c) $i_U = 0.7 \text{ pu}$ $i_o = 0.6 \text{ pu}$
 $i_L = 0.5 \text{ pu}$



(d) $i_U = 0.7 \text{ pu}$ $i_o = 0.7 \text{ pu}$
 $i_L = 0.65 \text{ pu}$

Fig. 8. Output waveforms obtained from analog computer set-up

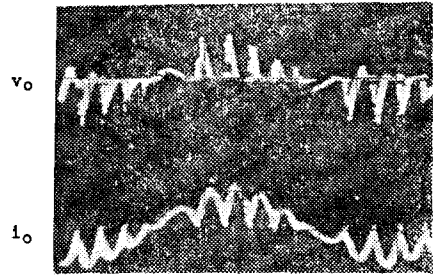


Fig. 9. Output waveforms obtained from the practical power circuit ($i_o = 0.2 \text{ pu}$)

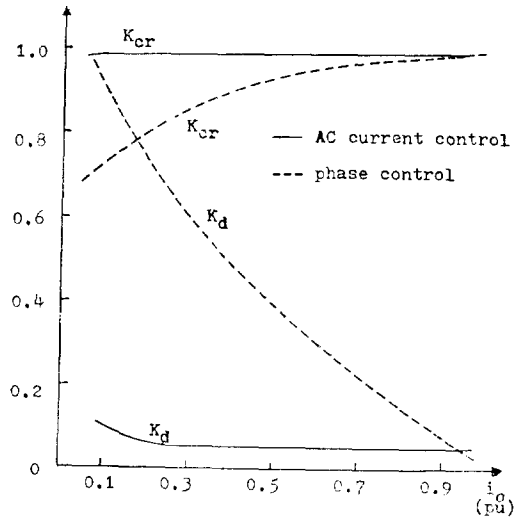


Fig. 10. Curves which compare AC current control with phase control under the same load condition

schmitt triggers used as the comparator compare the load current with the limit currents i_U and i_L and generate the ON or OFF signals. To turn off thyristor, Jones chopper circuit is modified to be suitable for AC current controlled system (Fig. 1-a) and the free wheeling thyristors are used as the free wheel path to prevent from being the short-circuit.

The outputs from the practical circuit are shown in Fig. 9.

V. Conclusions

Discontinuous load current and large harmonic

contents are disadvantages of load control by the phase control scheme. AC current control scheme is the multiple ON-OFF control method using the limit currents composed of sine wave. Fig. 10 shows the curves which compare the AC current controlled system with the phase controlled system under the same condition, i.e., the constant R-L load (in case of the phase angle $\phi=30^\circ$).

This control scheme can be found as follows:

- 1) The load current can be made continuous.
- 2) AC current controlled system can be operated irrespective of the phase angle ϕ while phase control is restricted to the range greater than the phase angle.

3) Decreasing the upper limit current, the ratio of the peak to rms current can be reduced.

4) A lower value of i_{DF} increases more switching losses per each half cycle but it reduces the harmonic contents and the waveform of load current improves greatly.

Nomenclature

- V_m : Peak value of AC source
 v_0 : Load voltage
 i_0 : Load current
 i_U : Upper limit current
 i_L : Lower limit current
 I_{MU} : Peak value of upper limit current
 I_{ML} : Peak value of lower limit current

i_{DF} : Peak difference of limit currents

R : Load resistance

L : Load inductance

ϕ : Phase angle of load $\left(\arctan \frac{\omega L}{R}\right)$

K_{cr} : Current ratio

K_d : Distortion factor

ω : Angular frequency of source (60Hz)

Reference

1. William Shepherd; "Steady-state Analysis of the Series Resistance-Inductance Circuit Controlled by Silicon Rectifiers," IEEE Trans. IGA, July/Aug. 1965.
2. Subhas K. Mukhopadhyay and Paresh C. Sen; "Current Control Scheme For solid state DC Motor Drives," IEEE Trans. Ind. Electron. Contr. Instrum., vol. IECI-20, No. 4, Nov. 1973
3. S.R. Doradla and Paresh C. Sen; "Solid state Series Motor Drives," IEEE Trans, Ind. Electron. Contr. Instrum., vol. IECI-22, No. 2, May 1975
4. S.B. Dewan and A. Straughen, Power Semiconductor Circuits, John Wiley & Sons, Inc., 1975
5. G. E., SCR Manual, G.E. Co., 1967